Nuclear Engineering and Technology xxx (xxxx) xxx

Contents lists available at ScienceDirect

Nuclear Engineering and Technology

journal homepage: www.elsevier.com/locate/net

Original Article

Concurrent operation of round beam and flat beam in a low-emittance storage ring

J. Lee [b], S. Ahn [b], J. Ko [a], B. Oh [a, **], G. Jang [b], Y.D. Yoon [b], S. Shin [a, *], J.-H. Kim [c], M. Chung [c]

[a] Department of Accelerator Science, Korea University, 2511 Sejong-ro, Sejong, 30019, South Korea
[b] Pohang Accelerator Laboratory, 768-1 Jigok-dong, Nam-gu, Pohang, Gyeongbuk, 37673, South Korea
[c] Ulsan National Institute of Science and Technology, Ulsan, 44919, South Korea

ARTICLE INFO

Article history:
Received 7 October 2022
Received in revised form
21 June 2023
Accepted 2 July 2023
Available online xxx

Keywords:
Round beam
4GSR
Radiation

ABSTRACT

In 4th-generation storage rings, whether to operate the beam as round or flat is a critical question. A round beam has equal horizontal and vertical emittances, and is an efficient solution to reduce strong intra-beam scattering effects and lengthen the Touschek lifetimes, but a flat beam produces a brighter photon beam than a round beam. To provide both beams concurrently rather than bifurcating the beam time, this paper presents the exploitation of beam dynamics and the cutting-edge fast pulser that supports concurrent operation of round beam and flat beam.

1. Introduction

Fourth-generation storage rings (4GSRs) are being developed rapidly. MAX-IV [1], SIRIUS [2] and ESRF [3] have successfully demonstrated the multi-bend achromat (MBA) lattice concept. Projects to upgrade existing third-generation storage rings (3GSRs) to 4GSRs (APS-U [4], ALS-U [5] and PETRA-IV [6]) are underway and a high-energy photon source (HEPS) [7] as a new 4GSR project is in progress. Many other 3GSRs are scheduled for upgrade to 4GSRs, and new 4GSR projects are being studied. The beam emittances for these facilities have been pushed down to a few hundred picometers or even <100 p.m.

When the emittance of a storage ring extremely small (i.e., ≤ ~100 p.m.), two primary consequences emerge: first, the dynamic aperture typically becomes insufficient to enable accumulation-based injection. Second, the increase in bunch density increases intra-beam scattering, and thus inevitably leads to a dramatic decrease in Touschek lifetime and increase in emittance. Particles within a bunch can collide with each other as they perform betatron and synchrotron oscillations. The collisions lead to a redistribution of the momenta within the bunch, and hence to a change in the emittances. A large change in momentum by large-angle scattering can lead to the energy deviation of particles becoming larger than the energy acceptance of the ring, in which case the particles are lost. This is the Touschek effect; it tends to be the dominant limitation on beam lifetime in low-emittance storage rings such as 4GSRs.

One efficient approach to reduce these effects is to operate such a machine in round-beam mode with equal horizontal and vertical emittances, because electron density is reduced in a round beam. Several methods to generate round beams in a storage ring have been proposed [8]: local emittance exchanger, damping wiggler with horizontal field, Mobius accelerator, and operation on the coupling resonance. Operating on the coupling resonance to obtain a round beam will most likely be the method of choice for many 4GSRs.

Typically the vertical emittance is well below the diffraction limit regime in a 4GSR. In the horizontal plane, emittance is already very close being diffraction-limited. Therefore, brilliance and coherence in the horizontal plane will be increased by generating a round beam. Users favor beam modes that are suitable for their respective experiments. A significant fraction of beamline users prefer round beams rather than flat beams in a light source [9]. However, some prefer a flat beam due to its high total brilliance, and some beamline users who use monochromators that have no entrance slit prefer flat beams as long as photon beam does not reach the diffraction limit fully.

* Corresponding author.
** Corresponding author.
E-mail addresses: obh96@korea.ac.kr (B. Oh), tlssh@korea.ac.kr (S. Shin).

https://doi.org/10.1016/j.net.2023.07.002

To satisfy various user requirements in a 3GSR, beam-time bifurcation is inevitable for certain purposes such as low-alpha-mode operation [10] and normal-mode operation, and various fill patterns (i.e., uniform fill patterns, a "several equally-separated bunch gap pattern" and a hybrid pattern in which the main bunch is separated by a long gap from long bunches). The situation is expected to be similar in 4GSRs, i.e., beam time bifurcation would solve the anticipated preference discrepancies among users.

To solve this problem, we demonstrate a new scheme that operates round and flat beams concurrently. This method is achieved using cutting-edge technology and exploiting the characteristics of beam dynamics. Section 2 introduces a linear analysis of a coupled lattice. Section 3 and 4 describe results on generating round beam and simulating off-axis injection in Korea-4GSR, respectively. Section 5 presents the scheme to concurrently operate round beams and flat beams, and describes a newly-developed short pulse-power supply. Section 6 gives a summary and conclusion.

2. Linear analysis of coupled lattice

In the linear approximation, the transfer matrix will have non-zero off-block-diagonal terms, which represent coupling among horizontal, vertical, and longitudinal motions. Such coupling is always presented in a storage ring, either as an intrinsic feature of the system, or by design, or as a result of imperfections in construction or tuning of the storage ring. Fig. 1 shows the generic one-turn transfer matrix including the off-diagonal betatron coupling and the dispersion terms. Vertical dispersion can be generated by machine imperfections such as quadrupole tilt errors, or vertical quadrupole and sextupole misalignments. An orbit distortion also gives a beam the same effects as magnet misalignment.

Vertical dispersion induced by these errors is given by [11].

$$\langle\frac{\eta_y^2}{\beta_y}\rangle = \frac{\langle\Delta Y_Q^2\rangle}{8\,sin^2\,\pi\nu_y}\sum_{quads}\beta_y(k_1L)^2 + \frac{\langle\Delta\Theta_Q^2\rangle}{8\,sin^2\,\pi\nu_y}\sum_{quads}\eta_x^2\beta_y(k_1L)^2 + \frac{\langle\Delta Y_S^2\rangle}{8\,sin^2\,\pi\nu_y}\sum_{sexts}\eta_x^2\beta_y(k_2L)^2, \quad (1)$$

where $\langle\Delta Y_Q^2\rangle$ is the mean square of vertical orbit distortion or vertical alignment errors on the quadrupoles, $\langle\Delta\Theta_Q^2\rangle$ is the mean square of tilts on the quadrupoles, and $\langle\Delta Y_S^2\rangle$ is the mean square of vertical orbit distortion or vertical alignment errors on the sextupoles. On the right-hand side of Eq. (1), the first term represents the skew dipole effect and the second and third terms represent the skew quadrupoles contributions.

Betatron coupling means that the vertical motion of a particle depends on its horizontal motion, and *vice versa*. This coupling effectively alters the horizontal and vertical emittances. In a storage ring, betatron coupling can arise from skew quadrupoles or magnet errors such as quadrupole tilt error and vertical alignment error. The coupled betatron motion can be solved using the perturbation theory of linear coupling resonance by assuming a weak skew field [11–13]. Using the perturbation theory without vertical dispersion, the ratio of the horizontal and vertical emittances in the presence of coupling, K, generated by weak skew quadrupoles can be derived as [11]

$$M = \begin{pmatrix} R_{11} & R_{12} & R_{13} & R_{14} & R_{15} & R_{16} \\ R_{21} & R_{22} & R_{23} & R_{24} & R_{25} & R_{26} \\ R_{31} & R_{32} & R_{33} & R_{34} & R_{35} & R_{36} \\ R_{41} & R_{42} & R_{43} & R_{44} & R_{45} & R_{46} \\ R_{51} & R_{52} & R_{53} & R_{54} & R_{55} & R_{56} \\ R_{61} & R_{62} & R_{63} & R_{64} & R_{65} & R_{66} \end{pmatrix}$$

Fig. 1. Generic one-turn transfer matrix with betatron coupling (red), horizontal dispersion (green) and vertical dispersion (blue) in storage ring.

$$K \equiv \frac{\varepsilon_y}{\varepsilon_x} = \frac{|C|^2}{\Delta^2 + |C|^2}, \quad (2)$$

where ε_x and ε_y are respectively the horizontal and vertical emittances, Δ is the difference in the fractional parts of the horizontal and vertical tunes, and

$$C = \frac{1}{2\pi}\oint k_s\sqrt{\beta_x\beta_y}e^{i\left(\phi_x-\phi_y-\frac{2\pi}{L}\Delta\right)}ds = |C|e^{i\phi_c}, \quad (3)$$

is the coupling driving term, where k_s is the skew quadrupole strength induced by quadrupole tilt errors or skew quadrupole errors alone, β_x and β_y are horizontal and vertical beta function, ϕ_x and ϕ_y are the horizontal and vertical betatron phase advances, respectively, and L is the ring circumference. When $K = 1$, emittance becomes

$$\varepsilon_x = \varepsilon_y = \frac{\varepsilon_{x0}}{1+\tau_x/\tau_y}, \quad (4)$$

where ε_{x0} is the natural beam emittance in a bare lattice without coupling, and τ_x and τ_y are respectively the horizontal and vertical damping times. If the ring does not have a skew quadrupole component, vertical emittance is generated by vertical quantum emission of synchrotron radiation with an angle proportional to $1/\gamma$, where γ is the relativistic factor of the beam. This emittance is very small compared to horizontal emittance. Thus, a major source of vertical emittance is betatron coupling, if it exists.

Eq. (2) demonstrate that emittance ratio must be in the range of 0–1. If K is small, the beam has a flat shape (flat beam) because of the small vertical emittance, and if K is close to 1, the beam has a round shape (round beam or fully-coupled beam) because horizontal and vertical emittances are similar. Also, Eq. (2) indicates that Δ should be minimized to increase K. It means that beam should be near difference resonance. Coupled lattice functions —$\beta_{xI}, \beta_{xII}, \beta_{yI}, \beta_{yII}$, … can be used to analyze the beam dynamics of betatron coupling [14,15]. In the uncoupled case ($K = 0$), $\beta_{xII} = 0$ and $\beta_{yI} = 0$, and in the fully-coupled case ($K = 1$) $\beta_{xI} = \beta_{xII} = \frac{\beta_x}{2}$ and $\beta_{yI} = \beta_{yII} = \frac{\beta_y}{2}$ [15].

Table 1
Major parameters of the Korea-4GSR storage ring.

Parameter	Value	Unit
Beam energy	4	GeV
Beam current	400	mA
Lattice structure	Hybrid 7BA	
Superperiods	28	
Natural hor. emittance	58	pm rad
Betatron tune	67.44/23.17	
RF frequency	500	MHz
Rms energy spread	0.12	%
Circumference	798.8	m

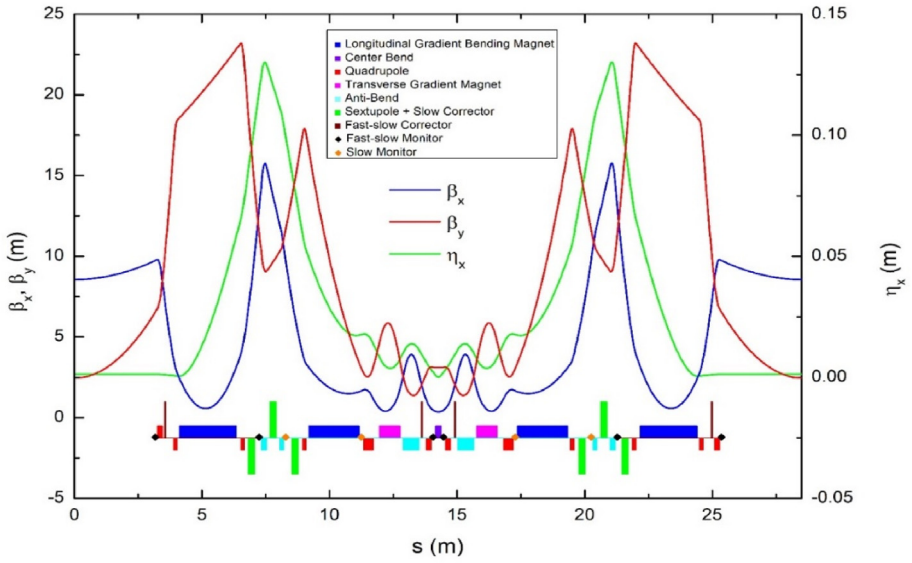

Fig. 2. Lattice functions for Korea-4GSR.

3. Realization of round beam in Korea-4GSR

3.1. Korea-4GSR

The lattice type of the Korea-4GSR [16] (Table 1, Fig. 2) was selected to be the hybrid multi-bend achromat type (HMBA) because it provides sufficiently low beam emittance with a good dynamic aperture. The ring is composed of 28 symmetrical cells which have a total circumference of 800 m, and the fiducial beam's natural emittance is 58 p.m. Each cell contains a 2-T high-field bend in the central dipole to produce radiation that has a critical energy of 21 keV.

The concepts behind the APS-U [17] and ESRF-EBS [18] lattices were adopted in the Korea-4GSR lattice. The dispersion was deliberately enlarged between the first and second dipoles and between the sixth and seventh dipoles. Chromatic sextupoles were located in these “dispersion-bump” regions to reduce the strength required to control the chromaticity. To naturally cancel non-chromatic effects of the sextupoles to first order, advances in the betatron phase between the two dispersion bumps were set to $\Delta\phi_x \sim 3\pi$ in the horizontal plane, and to and $\Delta\phi_y \sim \pi$ in the vertical plane.

3.2. Round beam in normal quadrupole with tilting error

Two cases to generate betatron coupling were investigated: (1) normal quadrupoles have tilt error, (2) skew quadrupoles are installed. In case (1), quadrupole tilt errors were generated using a Gaussian random number with standard deviation $\sigma = 1.1\times 10^{-4}$ with a condition that random numbers are produced in a range of $\pm 2\sigma$. The natural emittance of the Korea-4GSR is 58 p.m., with horizontal damping time of 11.1 ms, and vertical damping time of 21.1 ms. The calculated round beam emittance using Eq. (4) is 38 p.m. Beam tracking in the ring with tilted normal quadrupoles was performed using ELEGANT code [19] to verify round beam emittance. 5000 macro particles with 58-pm horizontal emittance and 5.8-pm vertical emittance (10% coupling) were created at the origin in a transverse plane and tracked for 30,000 turns (Table 2); both horizontal and vertical emittance converged on 38 p.m. after about 10,000 turns (Fig. 3).

Table 2
Condition of beam coupling simulation using normal quadrupole tilt errors.

Parameter	Value	Unit
Tilt error distribution	Gaussian	
σ_{tilt}	1.1×10^{-4}	radian
Number of titled quadrupoles per cell	6	
Number of macro particles	5000	
Turn number	30000	
Initial hor. emittance	58	pm rad
Initial ver. emittance	5.8	pm rad

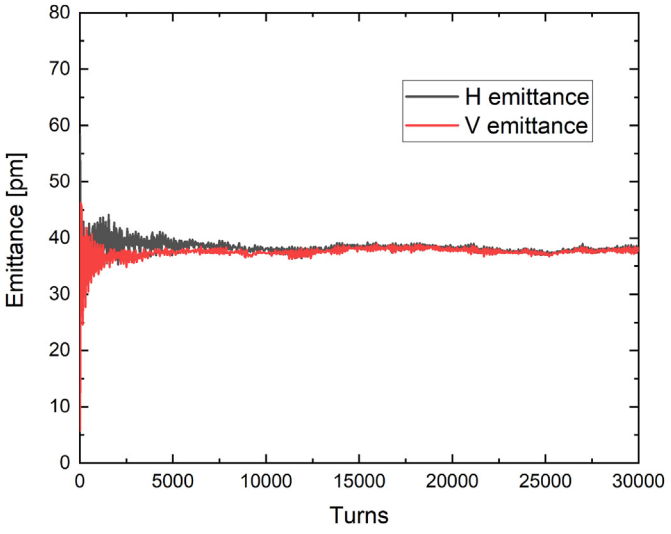

Fig. 3. Emittance variation from flat beam to round beam as a function of turn number. Quadrupole tilt errors were used for betatron coupling.

3.3. Round beam in skew quadrupole

According to Eq. (2), a round beam ($K = 1$) can be realized when $\Delta = 0$ at a given C or *vice versa*. To increase the coupling driving term C, a strong skew quadrupole strength can be considered in Eq. (3). But strong skew quadrupole strengths can trigger various side

effects such as unstable beam dynamics and high vertical dispersion. High vertical dispersion causes high vertical emittance. If we set skew component strengths k_s with constant value, then $|C|$ can be low because of oscillating term $\exp\left[i\left(\phi_x - \phi_y - \frac{2\pi}{L}\Delta\right)\right]$ in Eq. (3). To increase $|C|$, we must locate skew quadrupoles considering betatron phases. It will be a difficult to be adopted in the lattice design of storage ring. Instead, we can set k_s such that $k_s \propto sin\left(\phi_x - \phi_y - \frac{2\pi s}{L}\Delta\right)$. Then, from Eq. (3), below relationship can be established

$$C \propto \oint \sqrt{\beta_x \beta_y}\left[cos\left(\phi_x - \phi_y - \frac{2\pi s}{L}\Delta\right) + i \times sin^2\left(\phi_x - \phi_y - \frac{2\pi s}{L}\Delta\right) \times \right] ds. \tag{5}$$

Because $sin^2\left(\phi_x - \phi_y - \frac{2\pi s}{L}\Delta\right)$ is always positive, $|C|$ can be large with small $\sum |k_s|$.

When fractional tune separation is 0.005, the K is saturated from particular value of coupling driving term ($C \sim 0.005$) (Fig. 4a). To avoid harmful effects, K must be kept below the saturation value in the controllable tune separation range. Emittance ratio with various coupling driving term values vary with the fractional tune difference (Figure 4b); the fractional tune separation cannot be zero for various reasons, such as tune spread inside the bunch, and power supply noise. However, values < 0.005 are easily reachable.

To generate a round beam during operation, a skew quadrupole should be used rather than a quadrupole tilt error, because quadrupole tilt error cannot be controlled during beam operation. In Korea-4GSR, four skew quadrupoles are located at the dispersion-free region and six skew quadrupoles are used in combination with six sextupoles in the dispersion bumps. Therefore, a total of 10 skew quadrupole magnets are used to generate a round beam in cell. To obtain strong coupling while suppressing vertical dispersion (i.e., increase C while maintaining low skew quadrupole strengths), skew quadrupole strengths are generated along the given equation [20].

$$k_s = \frac{5 \times 10^{-4}}{\sqrt{\beta_x \beta_y}} \times \sin\left(\phi_x - \phi_y - \frac{2\pi s}{L}\Delta\right). \tag{6}$$

A round beam is generated with $C \sim 0.017$ at $\Delta = 0.001$, therefore, $K = 0.997$. Although $\Delta = 0.005$, which is easily reachable, $K = 0.92$. This K is sufficiently high to make full coupling beam. 5000 macro particles with initial $\varepsilon_x = 58$ p.m., $\varepsilon_x = 5.8$ p.m. (10% coupling) was generated at the origin in a transverse plane and tracked for 10,000 turns (Table 3) and their emittances converged to 38 p.m. in horizontal and vertical plane (Fig. 5). Beam life time was increased from 4.54 h to 8.81 h compared to bare lattice when RF voltage is 2.54 MV and beam current is 400 mA.

Beta functions of the bare lattice (β_x, β_y) and the coupled lattice (β_{xI}, β_{xII}, β_{yI}, β_{yII}) with the skew quadrupoles are shown in Fig. 6. Compared to the beta functions of bare lattice, each beta function of the coupled lattice became equal to half of bare beta functions (i.e., $\beta_{xI} = \beta_{xII} = \frac{\beta_x}{2}$ and $\beta_{yI} = \beta_{yII} = \frac{\beta_y}{2}$); these results imply that full coupling has occurred. In the dispersion functions (Fig. 7a), the vertical dispersion is uncoupled due to the small strength of the skew quadrupole because skew strengths are set as Eq. (6). If constant skew strengths are set, the vertical dispersion (Fig. 7b) is bumped along the cell due to large skew strengths. Bumped dispersion leads to a large equilibrium round-beam emittance of 70 p.m. Therefore, to realize a round beam that has small emittance, a strong skew quadrupole strength should be avoided.

4. Off-axis injection in round beam mode

Demonstration of off-axis beam injection in round beam mode is a crucial challenge in design studies of 4GSRs. Previous studies have demonstrated manageable off-axis injection in 3GSRs [21] and on-axis injection in 4GSRs [13], but demonstration of off-axis beam injection in 4GSR by using particle tracking is necessary in the round beam study as well as in the design study for 4GSR. In

Table 3
Condition of beam coupling simulation using lattice with skew magnets.

Parameter	Value	Unit
Skew strengths	$\frac{5 \times 10^{-4}}{\sqrt{\beta_x \beta_y}} \times \sin\left(\phi_x - \phi_y - \frac{2\pi s}{L}\Delta\right)$	
Number skew quadrupole per cell	10	
Number of macro particles	5000	
Turn number	10000	
Initial hor. emittance	58	pm rad
Initial ver. emittance	5.8	pm rad

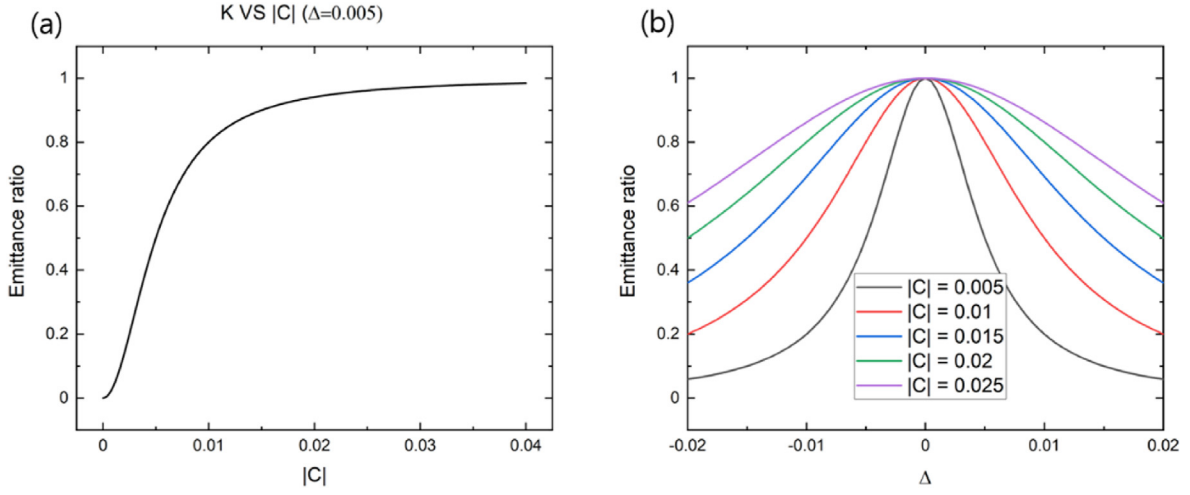

Fig. 4. Ratio of horizontal and vertical emittances along (a) coupling driving term and (b) tune separation.

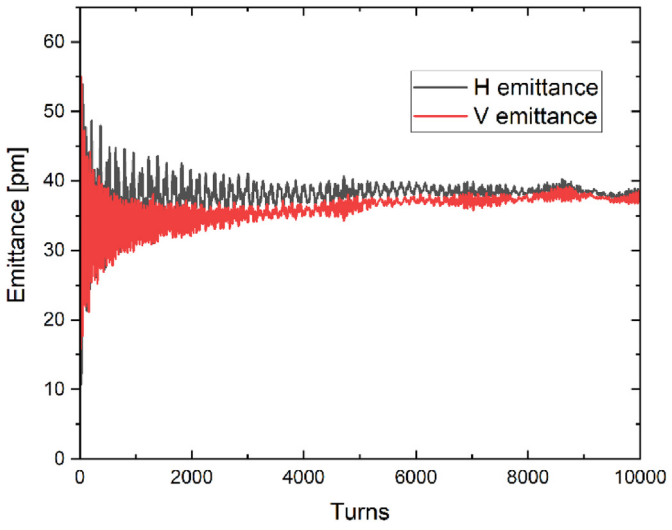

Fig. 5. Emittance variation from flat beam to round beam along as a function of turn number. Skew quadrupoles was used for betatron coupling.

general, to realize stable top-up operation in 3GSR, transverse coupling is suppressed to avoid beam losses due to large vertical beam oscillations at small apertures in, e.g., in-vacuum undulators. Large vertical beam oscillation in off-axis beam injection may be unavoidable in round beam mode, and may prevent the use of off-axis injection in round beam mode of the 4GSR. However, with large nonlinear detuning, high injection efficiency can be realized in a storage ring with full coupling, because the injected beam is shifted away from the coupling resonance [22]. This result should be verified by simulation for a ring with emittance <100 p.m.

The conventional four-kicker system is considered as the baseline off-axis injection system in Korea-4GSR, and a nonlinear single kicker system is considered as its alternative off-axis injection system. Although reference [13] shows beam injection in a small emittance ring, the beam had been simulated with on-axis injection system. The injection region includes four kickers for an orbit bump within a 6.5-m straight section. A kicker magnet can produce a 12-mm maximum bump height at 4-GeV electron-beam energy. The kicker magnet is operated at a 2-Hz repetition rate. It has a 3-μs half-sine wave so that the rise and fall times are both 1.5 μs The incoming electron beam from the beam-transfer line has the same vertical level as the bumped orbit in the storage ring and is injected 0.023 rad horizontally. The 3rd septum magnet then bends the beam −0.023 rad horizontally to make it parallel to the bumped orbit in the storage ring.

In Korea-4GSR, the booster ring and storage ring are concentric and share the same tunnel. Therefore, a small-emittance injected

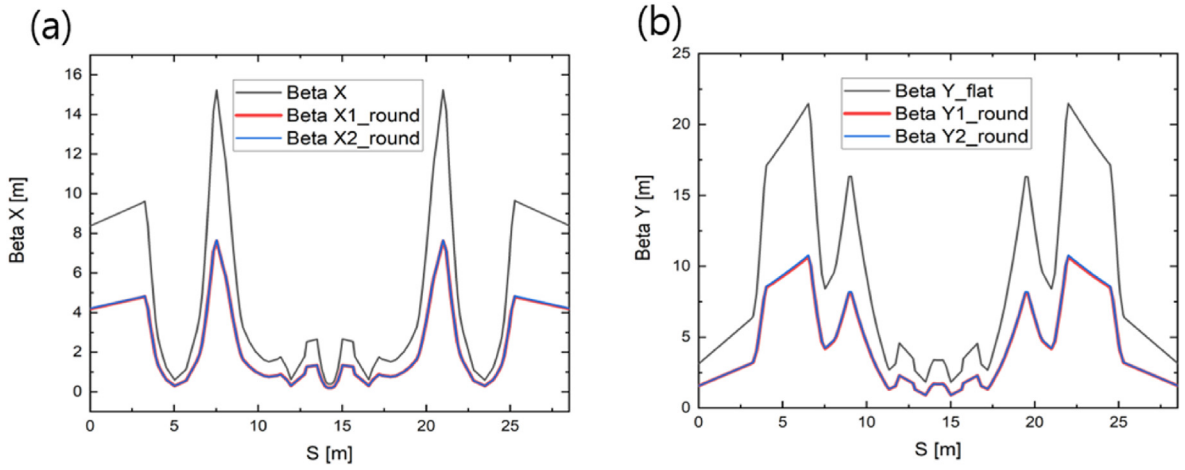

Fig. 6. Lattice functions comparison between bare lattice and coupled lattice for (a) horizontal plane and (b) Vertical plane.

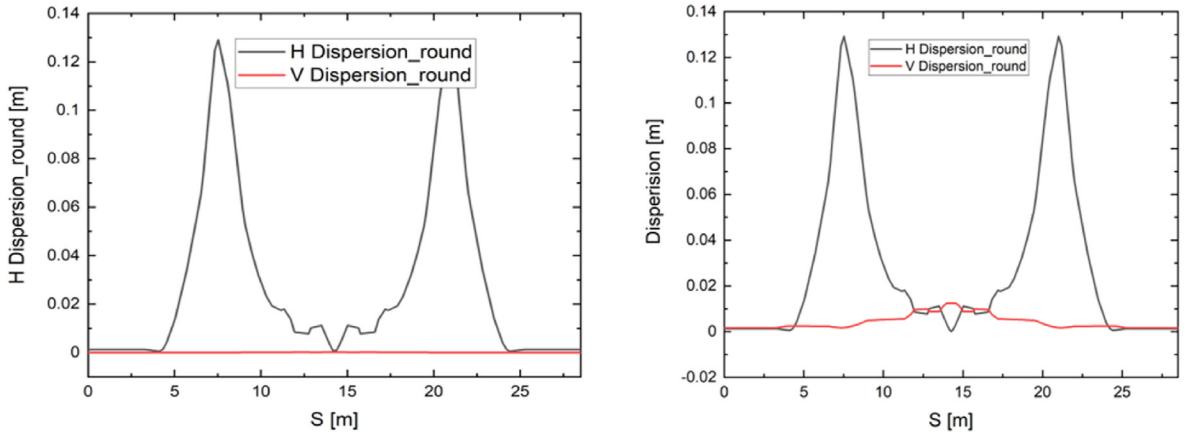

Fig. 7. Dispersion function of coupled lattice with (a) random skew quadrupole set and (b) constant skew quadrupole set.

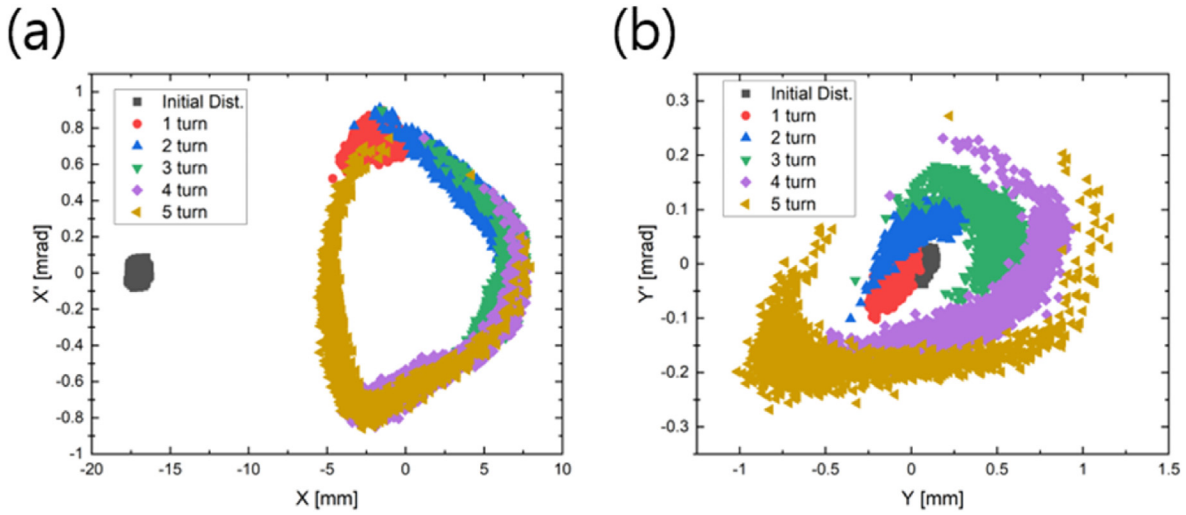

Fig. 8. Particle distributions during first five turns in phase space in (a) horizontal plane and (b) vertical planes.

beam can be available from the booster. Two different lattices have been designed for the booster; the natural emittance is 7 nm in one, and 1 nm in the other. However, only the injected beam parameter from the booster option with 7-nm natural emittance is considered in this study. To verify the beam injection in a round beam, multi-particle tracking with the ELEGANT code was performed for the round beam mode of Korea-4GSR. In the tracking, initial electron beam has the distribution with $\varepsilon_x = 7$ nm, $\varepsilon_y = 0.7$ nm, $\sigma_z = 6$ nm and $\sigma_\delta = 0.1\%$.

Three thousand particles with the initial electron beam dimensions were tracked for 30,000 turns, at which the beam distributions reached equilibrium values. In tracking studies, the septum clearance was reduced in the presence of nonlinear effects but it is still acceptable despite the high positive chromaticity that is necessary to suppress the head-tail instability. During the first five turns after injection, particles were spread out in horizontal phase space due to nonlinear effects from large horizontal beam offset (~5 mm) before sufficient damping occurs (Fig. 8a). Particles in vertical phase space also diverged from the initial distribution (Fig. 8b) due to coupling resonance effects, which transfer the horizontal oscillation energy to the vertical oscillation energy. In both round-beam mode (Fig. 9a) and flat-beam mode (Fig. 9b) the beam size evolved over time. In the round beam, the vertical beam size increased rapidly until 1500 turns then decreased to the equilibrium value. However, the maximum vertical beam size was still acceptable even in narrow vertical apertures such as the 5-mm full in-vacuum undulator gap.

5. Concurrent operation of round and flat beams

The several proposed methods to generate a round beam are not compatible with a flat beam. This section presents a method to concurrently operate round beams and flat beams. Korea-4GSR shows a large amplitude-dependent tune shift (ADTS) (Fig. 10), as do other low-emittance storage rings. Generally speaking, a large ADTS from strong sextupole strengths destroys stable beam motion by reducing the dynamic aperture. However, this nonlinear characteristic also has a positive effect on controlling a round beam.

Concurrent operation of round and flat beams exploits the effect of large ADTS to selectively control a specific bunch. Originally, short-pulsed quadrupole or skew quadrupole were considered to convert the specific bunch from flat beam to round beam or *vice versa*. For instance, a short-pulsed quadrupole moves the tune of the specific bunch far from coupling resonance in tune space, and thereby causes change to the characteristics of the emittance ratio. According to bunch-fill pattern, pulsed quadrupole or skew

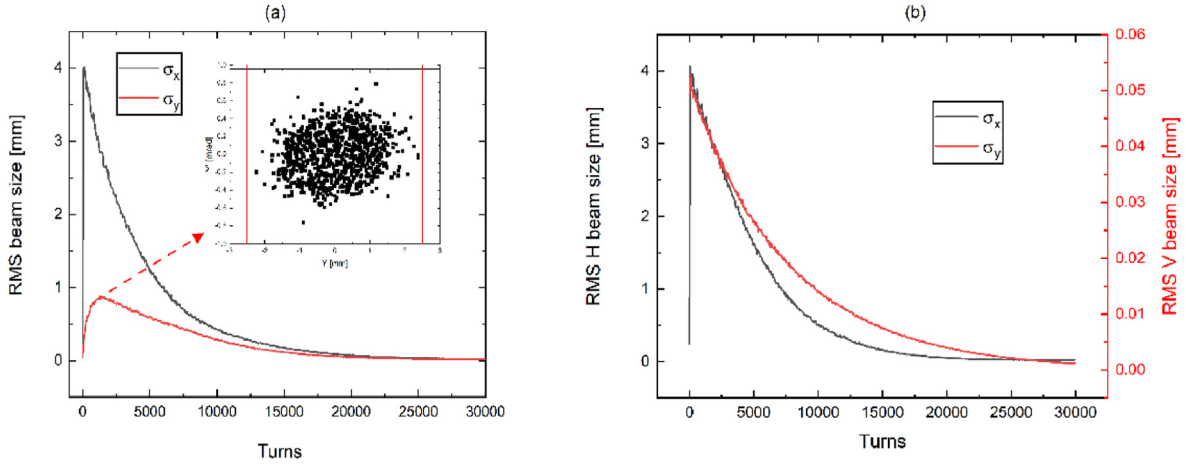

Fig. 9. Beam size along turns after injection in (a) round-beam mode and (b) flat-beam mode.

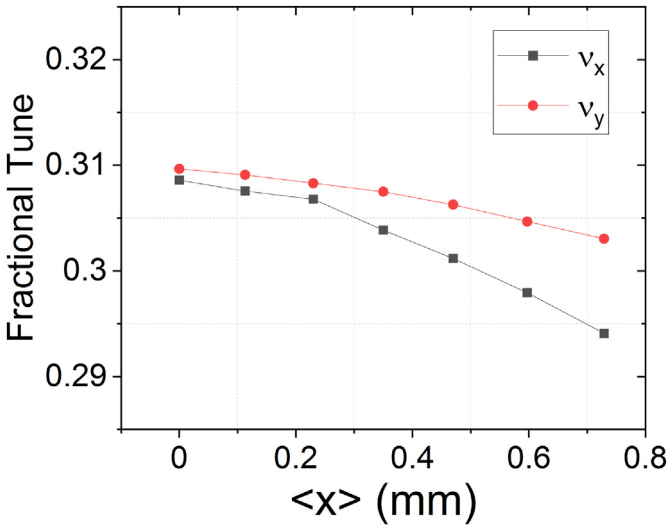

Fig. 10. Amplitude-dependent tune shift in Korea-4GSR.

Table 4
Major parameters of the nano-pulser which consists of four modules.

Parameter	Value	Unit
Max. voltage	40 (10 @ 1 module)	kV
Max. current	200	A
Rise time	10	ns
Fall time	8	
Pulse width	46–400	ns
Max. repetitive rate	500	kHz

quadrupole should require pulse duration of a few nanoseconds to a few tens of nanoseconds in this scheme. However, hardware for this system is not easy to realize. Instead of using the pulsed quadrupole or skew quadrupole, the pulsed dipole kicker is a good instrument to control the specific bunch with durations of a few nanoseconds to a few tens of nanoseconds.

The overall circuit (Fig. 11) of the proposed Solid-state Marx Modulator (SSMM) (Table 4, Fig. 12) includes several power cells. As shown in the figure, the SSMM has been successfully built and tested in the collaboration with Korea Institute of Electrical Research. Each power cell consists of three components: a storage capacitor ($C_{S-1} \sim C_{S-N}$), an ON switch ($S_{ON-1} \sim S_{ON-N}$) to generate pulses, and an OFF switch ($S_{OFF-1} \sim S_{OFF-N}$) to pull down the pulse and charge the storage capacitors. To transfer the gate signal and driving current of ON and OFF switches, one turn-control loop couples all the transformers ($TR_{G-1} \sim TR_{G-N}$) of gate drivers. The voltage of the control loop is applied by an On/Off pulse generator that uses a full-bridge inverter. The DC charger charges the storage capacitors in parallel through the charging diodes ($D_{charging-1} \sim D_{charging-N}$) and OFF switches. When ON switches are turned on, the charged storage capacitors are connected in series to apply the output pulse to the load.

To use the property of ADTS for concurrent operation of a round beam and a flat beam, consistent kick with the repetition rate of revolution frequency (375 kHz) should be selectively applied in the specific bunch. An orbit distortion of 0.75 mm can be expected by using the developed nano-pulse power supply satisfying 500 kHz maximum repetition rate. Only the selective bunches are steered in hybrid fill pattern, in which two long bunch train are separated by ion gap clearance. As result, 0.75-mm steered bunched shows different emittance ratio from round beam in undisturbed closed

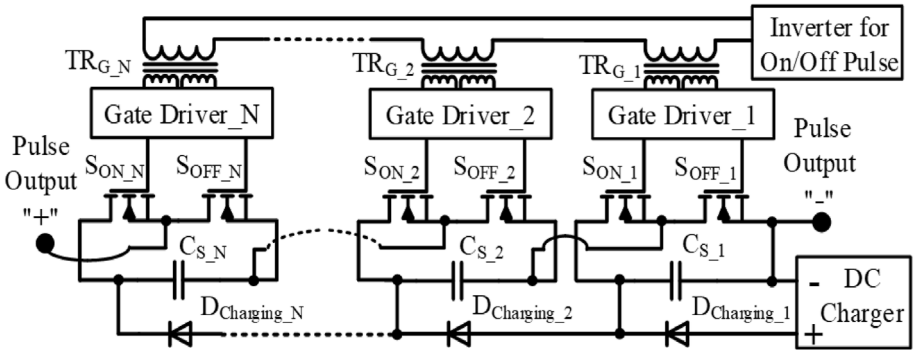

Fig. 11. Overall circuit based on power cell.

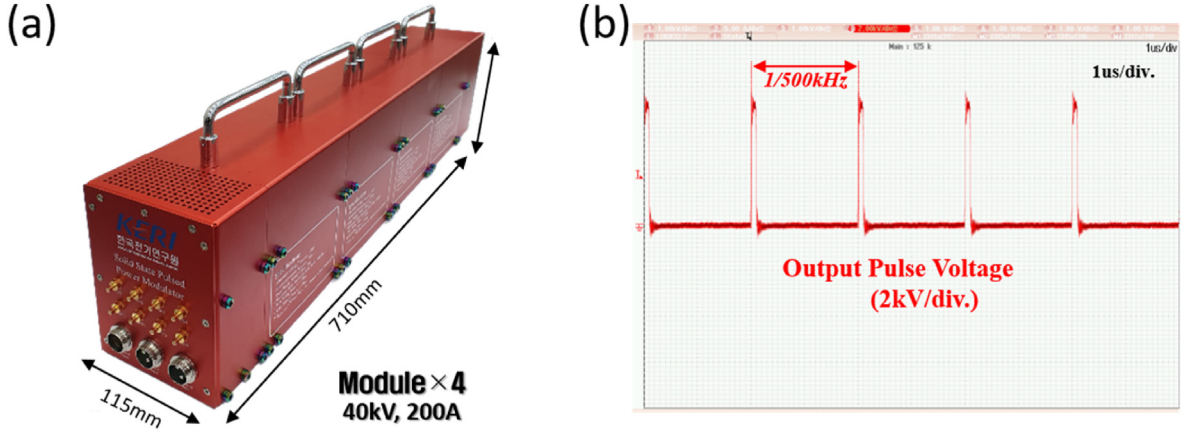

Fig. 12. Nano pulser. (a) Developed hardware. (b) Output pulse.

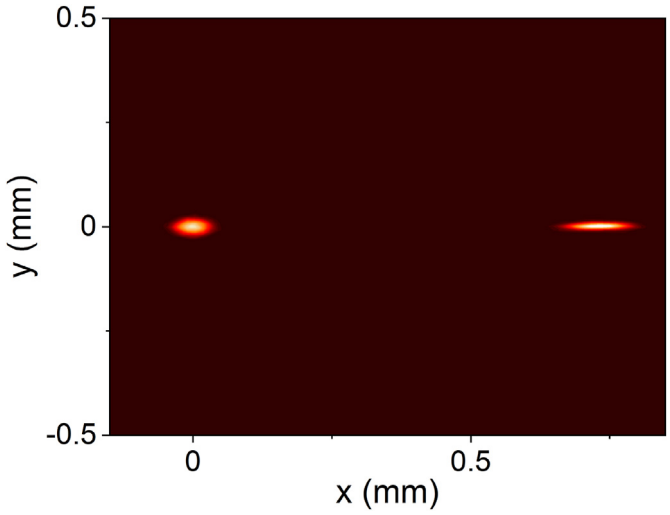

Fig. 13. Simulation results of concurrent operating mode of round beam and flat beam. Here, flat beam is selectively steered by the nano-pulse kicker system.

orbit. Simulation (Fig. 13) of concurrent operation on round beam and flat beam shows two long bunch trains that have different vertical closed orbits that spatially separate the light from bunch train with a flat beam from the main round bunch train in the beamline.

6. Conclusion

This paper has presented and simulated concurrent operation of round beam and flat beam for a fourth-generation storage ring. To generate a round beam, skew quadrupole magnets are set with small strengths without dispersion coupling to prevent vertical emittance increase due to vertical dispersion. Off-axis beam injection is also simulated in round beam mode. Maximum vertical beam size during injection transient is still within ±2.5 mm aperture in straight section for insertion device. Beam-time bifurcation between round beam and flat beam can cause inconvenience users when scheduling beam time. To solve this problem, the new scheme to operate concurrent round beam and flat beam is demonstrated by considering a nanosecond pulsed power supply and amplitude-dependent tune shift due to nonlinear effects.

Data availiability

The datasets used and/or analyzed during the current study available from the corresponding author on reasonable request.

Declaration of competing interest

The authors declare that they have no known competing financial interests or personal relationships that could have appeared to influence the work reported in this paper.

Acknowledgments

We would like to thank Michael Borland for providing helpful information and many useful discussions through elegant forum. This research was supported in part by the Korean Government MSIT (Multipurpose Synchrotron Radiation Construction Project) and also by Basic Science Research Program through the National Research Foundation of Korea (NRF-2019R1A2C1004862).

References

[1] MAX IV Conceptual Design Report, http://www.maxlab.lu.se/maxlab/max4/index.html.
[2] L. Liu, N. Milas, A.H.C. Mukai, X.R. Resende, A.R.D. Rodriguet, F.H. Sa, Proc. of IPAC (2013) 1874.
[3] ESRF-EBS introduction. http://indico.psi.ch/conferenceDisplay.py?confId=5589.
[4] APS Upgrade introduction. https://www1.aps.anl.gov/aps-upgrade.
[5] C. Steier, et al., Proc. of IPAC (2016) 2956.
[6] I. Agapov, et al., Proc. of IPAC (2019) 1404.
[7] HEPS introduction. http://english.ihep.cas.cn/heps/.
[8] Peter Kuske, Review of Methods to Produce Round Beams, Worksshop on Round Beams, SOLEIL, Paris, 2017.
[9] M. Aiba, M.P. Ehrlichman, A. Streun, Round beam operation in electron storage rings and generalisation of Mobius accelerator, Proc. of IPAC (2017) 1716.
[10] Xiaobiao Huang, et al., Low alpha mode for SPEAR3, Proc. of PAC07, pp. 1308.
[11] David Newton, Wolski Andy, Design of Electron Storage and Damping Rings USPAS, June 2013. Fort Collins, Colorado.
[12] H. Wiedemann, Particle Accelerator Physics, Springer, New York, 2015.
[13] Chongchong Du, Jiuqing Wang, Daheng Ji, Saike Tian, Studies of round beam at HEPS storage ring by driving linear difference coupling resonance, Nucl. Instrum. Methods A 976 (2020), 164264.
[14] F. Willeke, G. Ripken, Physics of particle accelerators, in: Melvin Month and Margaret Dienes, AIP Conf. Proc. No. 184, AIP, New York, 1989.
[15] F. Willeke, G. Ripken, On the impact of linear coupling on nonlinear dynamics, Part. Accel. 27 (1990) 203–208.
[16] G.S. Jang, S. Shin, M. Yoon, J. Ko, Dae Yoon Young, J. Lee, B.-H. Oh, Nucl. Instrum. Methods A 1034 (2022), 166779.
[17] Advanced photon source upgrade project final design report. https://publications.anl.gov/anlpubs/2019/07/153666.pdf.
[18] ESRF-EBS: the extremely brilliant source project. http://indico.psi.ch/conferenceDisplay.py?confId=5589.
[19] M. Borland, Elegant: a flexible SDDS-compliant code for accelerator simulation, Proc. ICAP-2000 LS-287 (2000).
[20] A. Chao, Handbook of Accelerator Physics and Engineering, World Scientific, Singapore, 2013.
[21] Tong Zhang, Xiaobiao Huang, Off-axis injection for storage rings with full coupling, Phys. Rev. Accel. and Beams 21 (2018), 084002.
[22] Masamitsu Aiba, Michael Ehrlichman, Andreas Streun, Round beam operation in electron storage rings and generalisation of Mobius accelerator, Proc. of IPAC (2015) 1716.